Journal of the European Ceramic Society 16 (1996) 561–5.

0955-2219(95)00161-1
0955-2219/96/$15.00

Sintering of Diphasic Mullite Gel

Ladislav Pach,[a] Aicha Iratni,[a] Vladimir Kovar,[a] Peter Mankos[a] & Sridhar Komarneni[b]*

[a]Slovak Technical University, Faculty of Chemical Technology, Department of Ceramics, Glass and Cement, 812 37 Bratislava, Radlinského 9, Slovakia
[b]Intercollege Materials Research Laboratory, The Pennsylvania State University, University Park, PA 16802, USA

(Received 23 March 1995; revised version received 10 August 1995; accepted 27 August 1995)

Abstract

A monolithic colloidal gel of mullite composition, prepared from SiO_2 and boehmite sols, was sintered under isothermal conditions. The sintering process was studied by dilatometry, thermogravimetric analysis, bulk density measurements and discontinuous shrinkage measurements. The silica component of stoichiometric colloidal mullite gel prevented crystallization of α-Al_2O_3 in the system. The initial rapid part of the sintering is controlled by the alumina phase and it is not a viscous sintering process in the sense of Scherer's viscous sintering model. The final part of sintering, above approximately 80% of the theoretical density, is controlled by the silica component of the gel and agrees very well with the Scherer model.

1 Introduction

The diphasic monolithic mullite gel is a precursor, which leads to mullite ceramics with a relative density above 96% at 1250–1350°C.[1–8] It is necessary initially to calcine the gel to prevent large volume changes from occurring during sintering.[9,10] The temperature at which the required sintering processes takes place is then increased at least to 1600°C. Many quantitative studies are related to this phenomenon, such as crystallization of mullite,[11–13] phase composition,[2,14,15] sintering of crystallized mullite[9,10] and mechanical properties of mullite ceramics.[1,9,16] Sintering of the gel (amorphous phase, before crystallization of mullite) is considered to be a simple process (viscous flow or viscous deformation mechanism)[3–5,18,19] and, therefore, it has received less attention in the overall study of mullite crystallization and densification. Generally it is believed that sintering of colloidal mullite gels takes place due to the silica component of this gel. But the process has not been analysed from the view point of the role of the individual components of the gel. In this work we shall try to resolve this question.

Sintering of colloidal gels such as silica or mullite is complicated in comparison with powdered glass, because water escapes from the gel during sintering, leading to an increase in viscosity.[19] The relation between OH content in the gel and the rate of sintering, however, is not yet fully understood.[19]

This work describes the sintering kinetics of diphasic mullite gels in correlation to Scherer's viscous sintering model[19,20] as determined by the weight loss of gels at annealing, the role of silica and alumina components during sintering of a mullite gel, the pore size distribution, and the high isostatic densification (at pressure of 1·5 GPa) of gel.

The Scherer model assumes a cubic array of interconnecting glass cylinders. The microstructure of the gel is represented by a unit cell with edge length l and a cylinder with radius a. The equation relating time to density of sample is:

$$\frac{\gamma}{\eta l_0}\left(\frac{\rho_S}{\rho_0}\right)^{1/3}(t - t_0) = \int_0^x \frac{2\mathrm{d}x}{(3\pi x^2 - 8\sqrt{2}x^3)^{1/3}} \quad (1)$$

where

$$x = a/l \quad (2)$$

$$8\sqrt{2}x^3 - 3\pi x^2 + \rho/\rho_S = 0 \quad (3)$$

γ is surface energy, ρ is density at time t, ρ_S is theoretical density, ρ_0 is initial density, η is the viscosity of the gel and t_0 is the fictitious time at which $x = 0$.

2 Experimental Procedure

Monolithic colloidal gels with the stoichiometry $3Al_2O_3.2SiO_2$ were prepared from commercial boehmite (Condea, ~10 nm particle size) and silica

*To whom correspondence should be addressed.

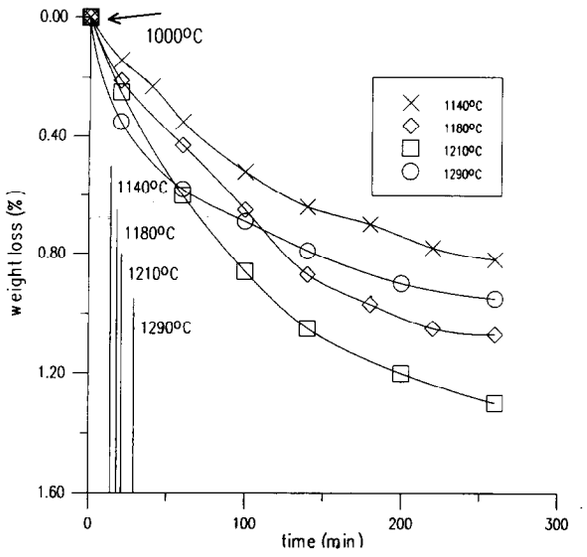

Fig. 1. Thermogravimetric analysis of diphasic mullite gels heated at the rate of 10°C min^{-1} and isothermal annealings. Weight changes of gel have been recorded from temperature 1000°C (standardized stage). Isothermal temperatures are achieved at indicated times with vertical lines on x-axis (time).

sol (Tosil, 30 wt% SiO_2, pH ≈ 9, particle size ≈ 12 nm, stabilized by NH_3). An aqueous boehmite dispersion (18 wt%) was peptized by mixing it with HNO_3 (pH ≈ 2), at 55°C. The boehmite sol was intensively mixed as the silica sol was slowly added. The mixed sol gelled within 1 h in a pan on a hot plate at about 80°C. The nearly transparent gels were extruded to rods (d ≈ 0.5 cm, l ≈ 5 cm). The monolithic gel rods were allowed to dry in air in a vertical position in order to retain their circular cross-section and shape. Dried gel rods were calcined at 550°C for 2 h. For the pressed samples, each gel rod was separately encapsulated and cold isostatically pressed at 1·5 GPa. Shrinkage of the gel rods (l = 2 cm, d = 0·5 cm) was measured during sintering using a Netsch 402 - E dilatometer at a heating rate of 10°C min^{-1} or by the discontinuous method. Rods of gels (l = 1 cm, d = 0·1 cm) were put suddenly into an oven (temperature range 1120–1220°C) and after sintering were quenched. Temperature change was about 600°C min^{-1} in the heating process. Thicker gel rods cannot be used because they disintegrated during the sudden heating. The lengths of the gel rods were measured before and after heat treatment using a micrometer. Relative density (ρ/ρ_S) curves reported in various figures were obtained from continuous dilatometric curves, thermogravimetric curves (Fig. 1) and bulk density measurements (liquid displacement method) with an error of ± 0·05 Mg m^{-3}. Relative density curves were then obtained from continuous dilatometric curves. Therefore, error bars cannot be introduced into figures.

3 Results

The specific surface area of the original gel (calcined at 550°C for 2 h) outgassed in vacuum at 350°C was 241 m^2 g^{-1}. The pore size was in a narrow range of 2–3 nm (unimodal pores). Upon isothermal heating of gels at 1140, 1180 and 1210°C [crystallization of mullite was not detected by X-ray diffraction (XRD)] and at 1290°C (mullite crystallized as detected by XRD) for 240 min, weight losses (Fig. 1) ranged from 0·8 to 1·3% compared with the standardized weight of a gel at 1000°C. If the gel is heated to the temperature at which crystallization takes place (e.g. 1290°C), the weight loss at the beginning is obviously faster than at a lower temperature, but later the weight loss is little or none as a consequence of crystallization of mullite. The standardized weight of the gels at 1000°C enables the gels to avoid the influence of physically adsorbed water (different humidity of air) on the measured weight changes.

Sintering of one-component gels (silica and alumina) and diphasic gels of mullite composition is shown in Fig. 2. Initial relative bulk densities ρ/ρ_O of gels increase in the order boehmite < mullite < silica gel. After sintering at 1220°C for 5 h the mullite gel yielded only defect (δ,θ)-Al_2O_3 phases. Mullite, however, did not crystallize. On the other hand, both the one-component gels crystallized. The boehmite gel totally transformed to α-Al_2O_3 and the silica gel partly crystallized to cristobalite.

Mullite sintering kinetics were analysed by Scherer's viscous sintering model.[19,20] Zero time of isothermal heating reported for the kinetics studies refers to that time at which the sample reached the isothermal temperature (Figs 3, 4 and 5). Theoretical curves generated by the solution of eqn (1) are shown by the solid line in Figs 3C, 4C and

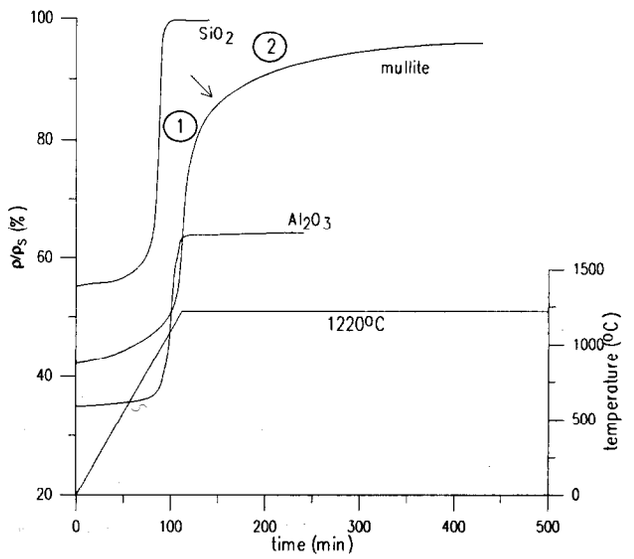

Fig. 2. Relative densities of silica, alumina and mullite colloidal gels vs. time of isothermal annealing at 1220°C: (1) the first part; (2) the second part of mullite densification.

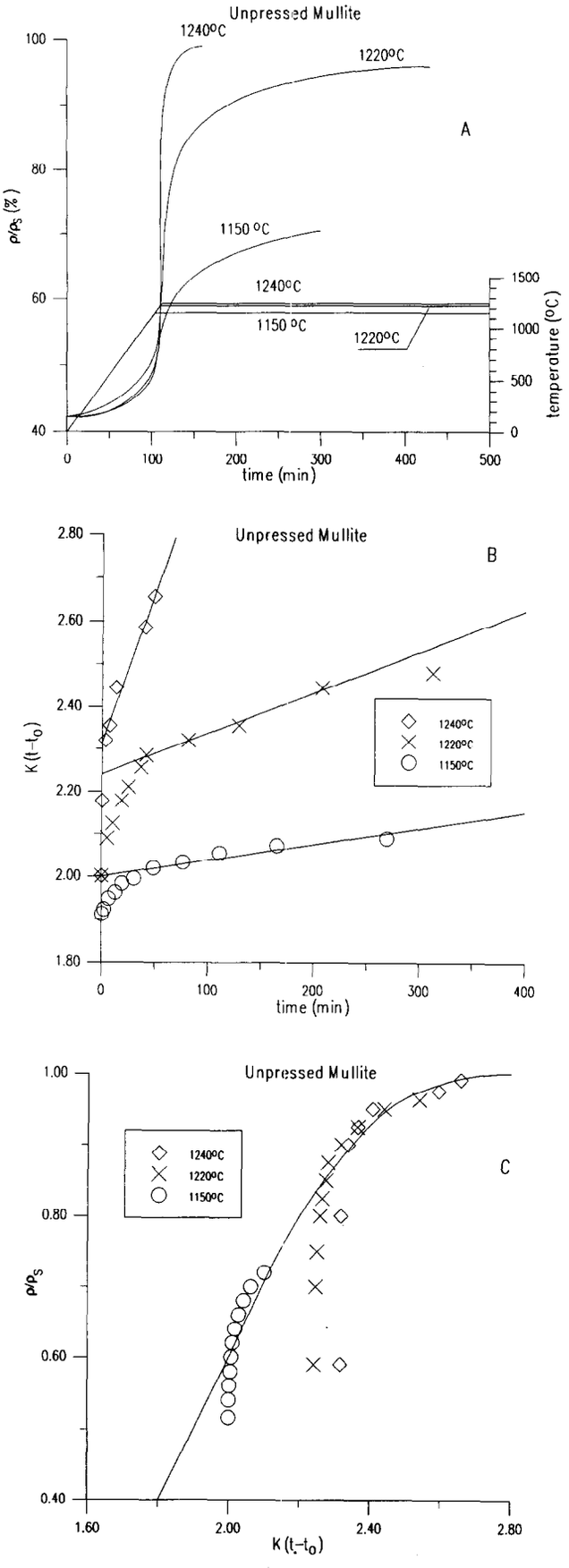

Fig. 3. Sintering of unpressed colloidal mullite gels at isothermal annealing temperatures of 1150, 1220 and 1240°C (increase of temperature 10°C min^{-1}).
A — relative bulk densities vs. time of isothermal annealing.
B, C — analysis of sintering kinetics by Scherer's model.
B — reduced time vs. experimental time.
C — relative bulk densities vs. reduced time, solid line is theoretical function of the model.

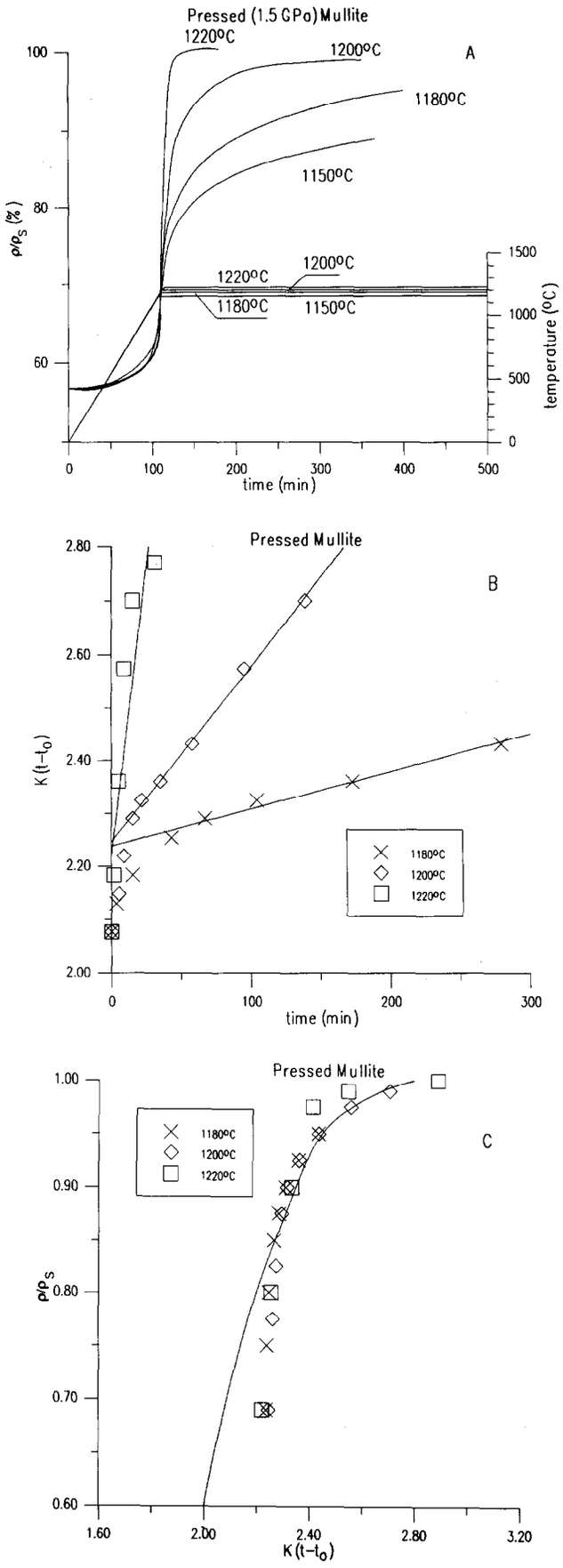

Fig. 4. Sintering of cold isostatically pressed (1·5 GPa) colloidal mullite gels at isothermal annealing temperatures of 1150, 1180, 1200 and 1220°C (increase of temperature 10°C min^{-1}).
A — relative bulk densities vs. time of isothermal annealing.
B — reduced time vs. time of experimental annealing.
C — relative bulk densities vs. reduced time, solid line is theoretical function of model.

5C. This function is used to find the reduced time $K(t - t_0)$ (where K is a constant, t is the experimental time and t_0 is a fictitious time at which $\rho = 0$) for experimental values of ρ/ρ_S. The function of these reduced times vs. the duration of isothermal heat treatment should be a straight line according to the model (Figs 3B, 4B and 5B) with slope:

$$K = \frac{\gamma(\rho_S/\rho_O)^{1/3}}{\eta l_O} \quad (4)$$

The length parameter of the model l_O can be calculated if the initial specific surface area S_O is known according to the following equation:

$$l_O = \frac{3}{S_O \rho_S x}\left(1 - \frac{\pi}{3\pi - 8\sqrt{2}x}\right) \quad (5)$$

Using eqn (5), initial relative density $\rho/\rho_S = 0{\cdot}42$ and surface area of 241 $m^2\ g^{-1}$, the length parameter of the Scherer model is 7·56 nm.

Gel viscosity was calculated from eqn (4). The required parameters K (slope of lines Figs 3B, 4B and 5B), l_O and ρ/ρ_O (Table 1) are available from the experimental measurements. For γ a value of 0·28 kJ m^{-2} was used.[19]

Initial steep parts of the sintering curves (Fig. 3A) for unpressed gels are not in agreement with theoretical functions of Scherer's model (Figs 3B and 3C). Disagreement increases with the increase in annealing temperature. In the case of the function $K(t - t_0)$ vs. time of isothermal annealing, disagreement with the model is in the deviation of experimental points from the straight line for short times (Fig. 3B). According to Scherer,[19] such deviation from the model represents an increase of viscosity caused by escape of water from the system. The above described relations for unpressed gels (Fig. 3) are nearly the same as those for cold isostatically pressed (1·5 GPa) gels (Fig. 4). However, the deviation from the model is smaller for the latter. Kinetic functions for rapidly heated samples (600°C min^{-1}) are shown in Fig. 5. Unlike the slowly heated samples (Figs 3 and 4), there is a broad agreement of experimental measurements with the model for rapidly heated samples. Kinetic parameters of gels are summarized in Table 1, and calculated functions of viscosities vs. $1/T$ are shown in Fig. 6 together with calculated activation energies. The activation energies are approximate because they were calculated based on only a few experimental points. The differences in activation energies clearly show that different processes are involved. All functions in Fig. 6 show two straight lines with different activation energies. Lines with low energies belong to viscous sintering of mullite gels without crystallization of mullite (mullite was not detected by XRD). Lines with

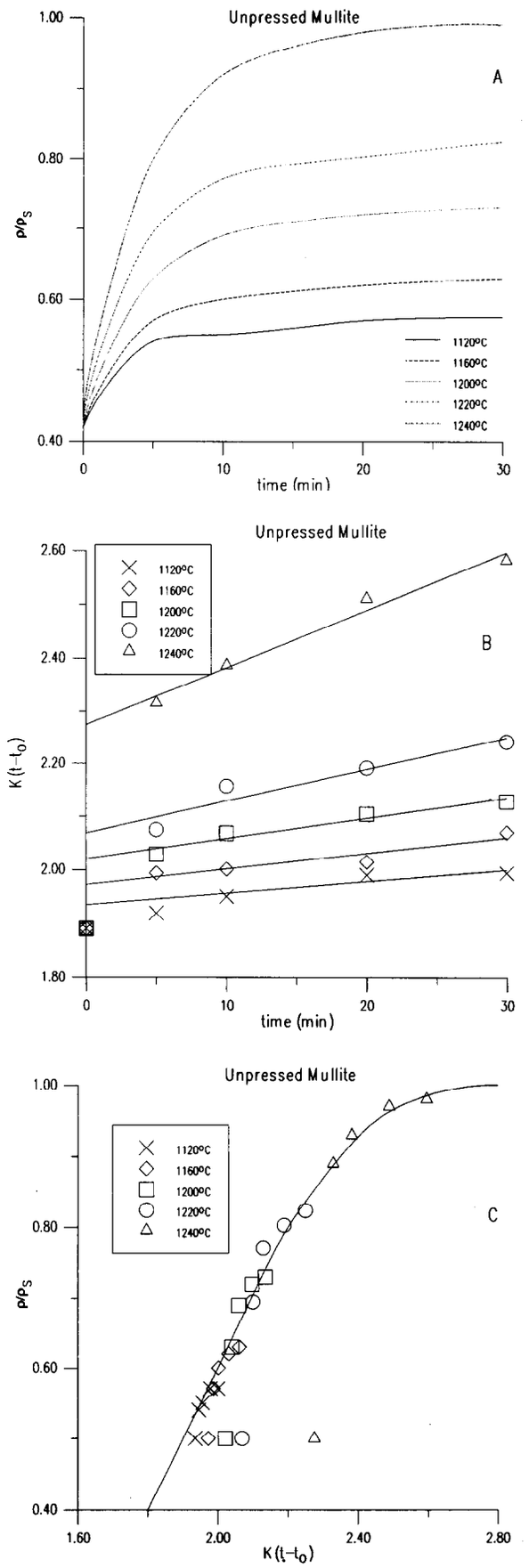

Fig. 5. Sintering of unpressed colloidal mullite gels at isothermal annealing temperatures of 1120, 1160, 1200, 1220 and 1240°C for rapidly heated samples (~600°C min^{-1}).
A — relative bulk densities vs. time of isothermal annealing.
B — reduced time vs. experimental time.
C — relative bulk densities vs. reduced time, solid lines are theoretical function of model.

Table 1. Kinetic parameters of sintering of diphasic colloidal mullite gels analysed by Scherer's model (K is constant of reduced time, viscosity is calculated for $l_0 = 7{\cdot}56$ nm, $\rho/\rho_S = 0{\cdot}42$ and $\gamma = 0{\cdot}28$ J m^{-2}; A — heating rate of ~600°C min^{-1}, B, C — heating rate of ~10°C min^{-1}; A, B — unpressed, C — pressed

Type	t *(°C)*	K *(s)*	η *(Pa.s)* $\times$ 10^{-12}
A	1120	$3{\cdot}6 \times 10^{-5}$	13·8
	1160	$4{\cdot}9 \times 10^{-5}$	10·1
	1200	$6{\cdot}3 \times 10^{-5}$	7·8
	1220	$10{\cdot}0 \times 10^{-5}$	4·9
	1240	$17{\cdot}8 \times 10^{-5}$	2·8
B	1150	$0{\cdot}6 \times 10^{-5}$	79·1
	1220	$1{\cdot}6 \times 10^{-5}$	30·9
	1240	$11{\cdot}6 \times 10^{-5}$	4·3
C	1150	$0{\cdot}7 \times 10^{-5}$	57·8
	1180	$1{\cdot}2 \times 10^{-5}$	41·7
	1200	$5{\cdot}6 \times 10^{-5}$	8·9
	1220	$36{\cdot}3 \times 10^{-5}$	1·4

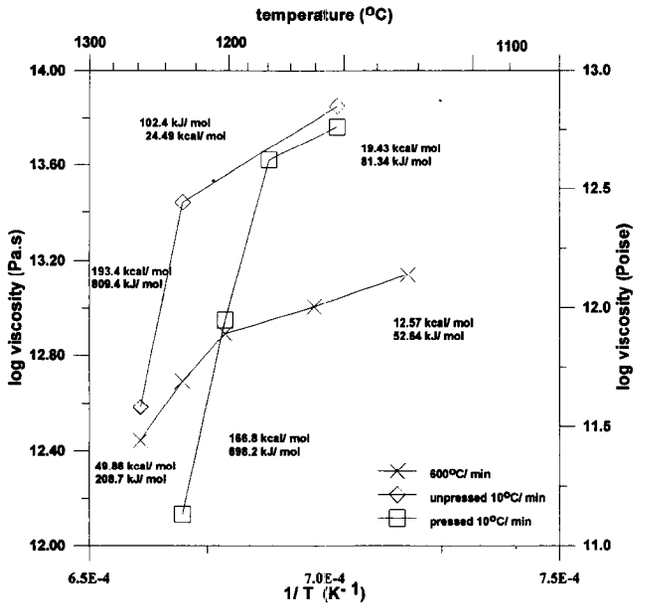

Fig. 6. Function of calculated viscosities (Scherer's model) vs. $1/T$ for diphasic mullite gels. Activation energies were calculated using an Arrhenius-type equation.

high energies belong to sintering and simultaneous crystallization of mullite. The sintering process in rapidly heated samples (600°C min^{-1}) takes place at significantly lower activation energies than in slowly heated samples (10°C min^{-1}). It is as a result of actual OH content in the samples, which can be assumed to be higher in rapidly heated samples.

4 Discussion

The diphasic mullite gel used here is composed of AlOOH or alumina particles (the latter present at temperatures >550°C), of size ~10 nm, and SiO_2 particles with size of ~11 nm. Considering stoichiometric mullite composition, a boehmite density of 3·70 Mg.m^{-3},[21] a silica density of 2·20 Mg m^{-3} and the above-mentioned particle size, the ratio of silica to boehmite (alumina) particles is 1:2·7. This means that the system is composed of 27% of silica particles and 63% of AlOOH particles (above 550°C alumina particles of the anhydrous type). Up to the temperature of intensive sintering both types of particles (i.e. silica and alumina) should form a connected network according to the percolation theory, which states that the threshold concentration to establish a connected network is about 16 vol% for a random mixture of two types of spherical particles of equal size.[22,23] This idea can be discussed by comparing the dilatometric curves of the one-component colloidal gels (SiO_2 and AlOOH) and of the diphasic gel of mullite stoichiometric composition (see Fig. 2). The silica gel used here becomes fully dense by 950°C, but the boehmite gel practically did not sinter below 1000°C. Slow sintering of the mullite gel up to about 1000°C is a result of sintering of the connected network of silica particles, leading to isolated islands of the SiO_2 phase. Above a temperature of 1000°C, sintering of boehmite derived gel is identical with sintering of the mullite gel (Fig. 2, part 1 of mullite gel). In the case of the boehmite gel, sintering was suddenly arrested by crystallization of α-Al_2O_3. If crystallization of α-Al_2O_3 did not take place, then it could be assumed that densification of the boehmite gel would not stop at a relative density of ~62% (Fig. 2) and would be continued. Such conditions are fulfilled in the mullite gels, where only direct crystallization of mullite was observed at about 1240°C. From this result, it is suggested that fast sintering of a mullite gel (Fig. 2, part 1) is controlled by the alumina phase. At this stage of sintering probably only one connected phase is present—the alumina phase. Silica enables this sintering of alumina by preventing the α-Al_2O_3 crystallization in the gel. Other influences of silica components at this stage of sintering of mullite gels are not yet clear. Further study would be needed for a better understanding of the role of the SiO_2 phase at this stage of the mullite gel sintering.

The same conclusion follows from sintering kinetic analysis by Scherer's model. The initial fast sintering of mullite (Fig. 2, part 1) as discussed above shows significant deviation from the model (Figs 3, 4 and 5). This result also indicates that the process is not a viscous sintering process in the sense of the model, where matter flows as a continuum (connected network of bonds M–O–M). It is rather flow of particles, especially flow of alumina particles. For such small particles as are

involved in the present mullite gels, viscous flow of particles and reorganization of particles are probably identical processes. These processes are influenced by the OH group content in the samples, as follows from the sintering kinetics of slow (10°C min^{-1}, Figs 3 and 4) and rapidly heated (600°C min^{-1}, Fig. 5) samples. At fast heating, the actual OH content of the samples is higher, as is observed from faster sintering at lower activation energies (Fig. 6).

Sintering of the mullite gel above ~80% of relative density (Fig. 2, part 2), is much slower than below ~80% density (Fig. 2, part 1) and agrees very well with Scherer's sintering model. The SiO_2 phase now begins to control the sintering process by the well known[19,20] viscous flow sintering mechanism. The silica phase begins to form a connected network in the sense of Si–O–Si bonds, unlike the initial gel where it is necessary to consider a network of colloidal silica particles. It is enabled by the spreading of the Al_2O_3/SiO_2 interface at the cost of Al_2O_3/vapour and SiO_2/vapour interfaces. With the increased movement of ions at this stage, crystallization of mullite also takes place. In the studied gel the crystallization of mullite had occurred at 1240°C.

Activation energies of viscous flow obtained from the (model) slopes of linear functions of K $(t-t_0)$ vs. experimental time (Figs 3B, 4B and 5C) depends on temperature, pressing and also on the heating rate (Fig. 6). The activation energies decrease as follows: unpressed gel > pressed gel > fast heated gel. These processes are significantly influenced by actual OH concentration in the sample and by crystallization of mullite.

5 Conclusion

The silica component of stoichiometric colloidal mullite gels prevents the crystallization of α-Al_2O_3. It enables the alumina component of the gel to control the sintering of the mullite gel by means of a connected network of (δ,θ)-Al_2O_3. The initial fast part of sintering is not a viscous sintering process in the sense of Scherer's sintering model. The second, slow part of sintering, above about 80% of theoretical density is controlled by the silica component of the gel and agrees very well with Scherer's model. The sintering process and also the activation energies are influenced by the rate of temperature increase, apparently as a consequence of an actual OH content in the gels.

Acknowledgement

This research was supported by NSF under grant No. 9001204.

References

1. Aksay, I. A., Dabbs, D. M. & Sarikaya, M., *J. Am. Ceram. Soc.*, **74** (1991) 2343.
2. Wang, Y., Li, D. X. & Thompson, W. J., *J. Mater. Res.*, **8** (1993) 195.
3. Komarneni, S., Suwa, Y. & Roy, R., *J. Am. Ceram. Soc.*, **69** (1986) C-155.
4. Yoldas, B. E., *Am. Ceram. Soc. Bull.*, **59** (1980) 479.
5. Jeng, D.-Y. & Rahaman, M. N., *J. Mater. Sci.*, **28** (1993) 4904.
6. Mroz Jr, T. J. & Laughner, J. W., in *Ceramic Transactions, Vol. 7, Sintering of Advanced Ceramics*, ed. C. A. Handwerker, J. E. Blendell and W. Kaysser. American Ceramic Society, Westerville, OH, 1990, pp. 664–70.
7. Rahaman, M. N. & Jeng, D.-Y., in *Ceramic Transactions, Vol. 7, Sintering of Advanced Ceramics*, ed. C. A. Handwerker, J. E. Blendell and W. Kaysser. American Ceramic Society, Westerville, OH, 1990, pp. 753–66.
8. Wu, J., Chen, M., Jones, F. R. & James, P. F., *J. Non-Cryst. Solids*, **162** (1993) 197.
9. Hirata, Y., Sakeda, K., Matsushita, Y., Shimada, K. & Ishihara, Y., *J. Am. Ceram. Soc.*, **72** (1989) 995.
10. Mroz Jr, T. J. & Laughner, J. W., *J. Am. Ceram. Soc.*, **72** (1989) 508.
11. Wei, W. & Halloran, J. W., *J. Am. Ceram. Soc.*, **71** (1988) 166.
12. Wei, W. & Halloran, J. W., *J. Am. Ceram. Soc.*, **71** (1988) 581.
13. Sundaresan, S. & Aksay, I. A., *J. Am. Ceram. Soc.*, **74** (1991) 2388.
14. Li, D. X. & Thompson, W. J., *J. Mater. Res.*, **6** (1991) 819–24.
15. Hulling, J. C. & Messing, G. L., *J. Non-Cryst. Solids*, **147–148** (1992) 213.
16. Dokko, P. C., Pask, J. A. & Mazdiyasni, K. S., *J. Am. Ceram. Soc.*, **60** (1977) 150.
17. Shinohara, N., Dabbs, D. M. & Aksay, I. A., *SPIE Vol. 683, Infrared and Optical Transmitting Materials* (1986) 19–24.
18. Sonuparlak, B., *Adv. Ceram. Mater.*, **3** (1988) 263.
19. Scherer, G. W., Brinker, C. J. & Roth, E. P., *J. Non-Cryst. Solids*, **72** (1985) 369.
20. Scherer, G. W., *J. Am. Ceram. Soc.*, **60** (1977) 236.
21. Wilson, S. J. & Stacey, M. H., *J. Colloid Interface Sci.*, **82** (1981) 507.
22. Sacks, M. D., Bozkurt, N. & Scheiffele, G. W., *J. Am. Ceram. Soc.*, **74** (1991) 2428.
23. Zallen, R., *The Physics of Amorphous Solids*. Wiley, New York, 1983, pp. 183–91.